Surface-Analytical Studies of Supported Vanadium Oxide Monolayer Catalysts

Laura E. Briand,[†] Olga P. Tkachenko,[‡] Monica Guraya,[§] Xingtao Gao,[⊥] Israel E. Wachs,[⊥] and Wolfgang Grünert*

Lehrstuhl für Technische Chemie, Ruhr-Universität Bochum, D-44780 Bochum, Germany, Centro de Investigación y Desarrollo en Ciencias Aplicadas, UNLP, CONICET, 47 No. 257, B1900AJK La Plata, Buenos Aires, Argentina, and Operando Molecular Spectroscopy and Catalysis Laboratory, Department of Chemical Engineering, Lehigh University, Bethlehem, Pennsylvania 18015

Received: December 2, 2003

Supported vanadium oxide catalysts, consisting of surface vanadia species on Al_2O_3, ZrO_2, CeO_2, and Nb_2O_5 oxide supports, were investigated by X-ray photoelectron spectroscopy (XPS) and ion scattering spectroscopy (ISS) to elucidate the effect of calcination treatments as well as exposures to (nonmonochromatized) X-rays and He ions on the surface properties. It was found that calcination in air at 730 K of samples that had been previously calcined in air at 773 K and exposed to ambient atmosphere results in significant increases of the V intensity relative to the support signal both in XPS and ISS. This indicates that the surface vanadia species aggregate under the influence of moisture, but spread during calcination. The surface V(V) species were reduced to V(IV) upon extended exposure to X-rays of a nonmonochromatized source, which was accompanied by clustering as detected by ISS. Following a new methodology that avoids these effects by studying freshly calcined samples transferred without exposure to ambient atmosphere, without previous illumination by X-rays, and takes account of the abrasive effect of He ions by extrapolating the results of sputter series, it was found that in supported V_2O_5/ZrO_2, V_2O_5/CeO_2, and V_2O_5/Nb_2O_5 catalysts possessing a vanadia monolayer coverage or above, the supports are densely covered by two-dimensional surface vanadia species, and the underlying oxide support cations of Zr, Ce, or Nb are not exposed. For a supported V_2O_5/Al_2O_3 catalyst containing a monolayer surface coverage of vanadia, however, a slight exposure of the oxide support cation (Al^{3+}) was noted, which may originate from the much higher surface area of this support ($Al_2O_3 \gg Nb_2O_5$, ZrO_2, and CeO_2) resulting in a higher curvature of the surfaces covered by the supported vanadia species. The current XPS and ISS surface studies confirm that supported vanadium oxide catalysts consist of close-packed monolayers of surface vanadia species.

Introduction

Supported transition metal (TM) oxides are active catalysts for a variety of reactions, many of them of technological interest (e.g. selective oxidation of *o*-xylene to phthalic anhydride, selective reduction of nitrogen oxides by ammonia to nitrogen and water, selective oxidation and ammoxidation of C_2-C_4 hydrocarbons to olefins, oxygenates, and nitriles, metathesis of olefins). In recent years, considerable progress has been made in the fundamental understanding of these materials, but some questions are still under debate. It has been found by vibrational techniques, in particular Raman spectroscopy and IR spectroscopy to a lesser extent, that under ambient conditions the surface TM oxide species are detached from the surface and hydrated by adsorbed multilayers of water (typically clusters of vanadates, molybdates, tungstates, etc.).[1,2] Their structures depend on the net pH at the point of zero charge, which is determined by the support at low TM oxide content, but is increasingly influenced by the TM species at higher loadings. Only upon calcination, which desorbs the adsorbed water and decomposes the TM oxide clusters, do the TM oxide species bind to the support and form a two-dimensional overlayer of isolated and oligomeric surface species. It also has been concluded from these studies that transition metal oxide species (V, Nb, Ta, Mo, W, Cr) form a complete surface monolayer coverage on most oxide supports (with the exception of SiO_2). Above monolayer surface coverage, the formation of TM oxide crystallites is observed, with the exception of rhenium oxide[2,3] because of its volatility.

This view is at variance with earlier reports that concluded that a second layer or TM oxide crystallites can be formed in many systems before the first layer is completed (MoO_3/Al_2O_3,[4] V_2O_5/TiO_2,[5] V_2O_5/Al_2O_3,[6] WO_3/TiO_2,[7,8] WO_3/ZrO_2[9]). If this is true, then the oxide support should be exposed to the gas phase to some extent in a catalyst with a loading equal to the theoretical monolayer surface coverage. Moreover, the multilayer model also implies that there is only a small excess of energy in the interaction between first layer and the oxide support over the interaction between second and first layers, hence, part of the support should be exposed even above monolayer surface coverage (cf. e.g. the analogue of molecular physisorption (multilayer) and chemisorption (monolayer)). This was claimed to be the case in several systems on the basis of ISS and CO_2 chemisorption data.[7,9,10]

In these discussions, the surface spectroscopies have largely contributed to the determination of the monolayer coverage (or the area requirement per transition metal oxide species). X-ray

* Address correspondence to this author at the Ruhr-Universität Bochum. Phone: +49-234-322-2088. Fax: +49-234 321-4115. E-mail: w.gruenert@techem.rub.de.
[†] Centro de Investigación y Desarrollo en Ciencias Aplicadas.
[‡] On leave from N. D. Zelinsky Institute of Organic Chemistry, Russian Academy of Sciences, Moscow, Russia.
[§] On leave from Centro Atomico Bariloche, CNEA, Argentina.
[⊥] Lehigh University.

10.1021/jp037675j CCC: $27.50
Published on Web 03/19/2004

TABLE 1: Properties of Supported Vanadium Oxide Catalysts Studied

code	composition, % V_2O_5	BET surface area (m^2/g)	surface V density (atoms/nm^2)	code	composition, % V_2O_5	BET surface area (m^2/g)	surface V density (atoms/nm^2)
1-V-Ce	CeO_2, 1.15	26.3	2.9	1-V-Zr	ZrO_2, 0.4_5	35.4	0.9
2-V-Ce	CeO_2, 1.6	28.6	3.7	2-V-Zr	ZrO_2, 1.8	35.7	3.3
3-V-Ce	CeO_2, 2.6	23.1	7.4	$(3\text{-V-Zr})_a$	ZrO_2, 2.6	34.4	5.0
5-V-Ce	CeO_2, 4.7	19.8	15.7	$(3\text{-V-Zr})_b$	ZrO_2, 3.3	34.2	6.4
6-V-Ce	CeO_2, 5.8	17.6	21.8	4-V-Zr	ZrO_2, 4.0	35.0	7.6
8-V-Al	Al_2O_3, 7.8	186.4 (202.2)[a]	2.8	6-V-Nb	Nb_2O_5, 6.1	55.2	7.4
15-V-Al	Al_2O_3, 15.3	169.8 (200.5)[a]	6.0				
24-V-Al	Al_2O_3, 23.7	162.3 (212.7)[a]	9.7				

[a] Surface per g of Al_2O_3.

photoelectron spectroscopy (XPS) only in rare cases indicates differences in the coordination state of species that are in an identical oxidation state, and it is therefore more frequently employed for reduction studies. With the oxidized state, its use is normally limited to comparisons between the surface and bulk metal/support ion ratio, which tends to yield a proportionality below the theoretical monolayer coverage and to level off or change to a smaller increase above this limit. These plots, however, are not suited to decide if the support becomes completely covered before a second monolayer is built up. Due to the average sampling depth of 1.5−2.5 nm (only ca. 30% of the signal intensity arises from the outermost sample layer) and the errors inherent in intensity evaluation, a considerable part of the TM oxide species could be deposited onto the first layer instead of the bare oxide support before a significant effect could be noted via the line intensities. In the study of real catalyst powders that exhibit curved surfaces, even the benefit from angular dependent XPS, which is well suited to improve surface sensitivity of XPS with flat samples,[11] will be limited.

On the other hand, ion scattering spectroscopy (ISS), which exclusively reflects the properties of the outermost surface layer, has been frequently employed to study supported transition metal oxide catalysts[10,12−14] and it has even been used to determine surface coverages quantitatively in combination with chemisorption techniques.[6,10,15] For alumina-supported metal oxide systems, this methodology was based on the quantitative use of the Al/O ISS intensity ratios that decrease with increasing transition metal oxide content. This ratio was often observed to level off at higher TM oxide content, sometimes even below the theoretical monolayer coverage, which was considered as proof for the beginning of multilayer formation.[6−9] In other cases, the support line was still observed at TM oxide contents clearly above the monolayer surface coverage.[10,13]

The history of the samples studied in the literature is not always clear: although a calcination of the samples is usually mentioned it is not obvious if these samples have been exposed to the humidity-containing ambient atmosphere prior to the surface-spectroscopic investigation or not. This is critical because rehydration should cause aggregation of the 2-dimensional layers of monomeric and polymeric transition metal oxide species into 3-dimensional aggregates (for the fully hydrated state, e.g., $V_{10}O_{28}\cdot H_2O$, $Nb_2O_5\cdot nH_2O$, $Mo_7O_{24}\cdot H_2O$). Furthermore, it has not always been appreciated that inappropriate impregnation methods for the TM oxide component (precursors with low solubility in the employed solvent or poor distribution of the precursor during the impregnation step) can result in the formation of microcrystalline TM oxide phases below monolayer surface coverage that may survive the calcination treatments employed without developing the full oxide−oxide interactions leading to monolayer formation.

The present investigation consists of a surface-spectroscopic examination of supported vanadium oxide catalysts that has been undertaken to analyze the oxide support exposure at monolayer surface coverage. The oxide supports included were Al_2O_3, ZrO_2, CeO_2, and Nb_2O_5. Unfortunately, the highly relevant TiO_2 support had to be excluded from this investigation due to the inability of normal ISS equipment to resolve the V and Ti signals. Significant differences were found between calcined catalysts investigated immediately after calcination (transfer into the spectrometer without exposure to ambient atmosphere: "in situ calcination") and after storage in the usual sample vessels exposed to humidity-containing ambient air. Moreover, it was observed that photoreduction of V(V) surface species during the preceding XPS analyses[16,17] also affects the apparent surface coverage. After taking account of all these complications, it can be demonstrated that the vanadium oxide forms a complete monolayer on ZrO_2, CeO_2, and Nb_2O_5 supports, which prevents detection of the oxide support cations. However, at monolayer coverage of surface vanadium on alumina the Al support ions remain visible to a very small extent, probably due to the greater curvature of surfaces exposed by the smaller alumina particles.

Experimental Section

Materials. Supported vanadium oxide catalysts were prepared by the incipient wetness impregnation of supports with solutions of vanadium triisopropoxide ($VO(O\text{-}Pr^i)_3$, Alfa, 95−98% purity) in methanol. The supports employed were Al_2O_3 (Engelhard, $S_{BET} = 222\ m^2/g$), ZrO_2 (Degussa, $S_{BET} = 34\ m^2/g$), CeO_2 (SKK company, $S_{BET} = 36\ m^2/g$), and Nb_2O_5 (Niobium Products Co., $S_{BET} = 57\ m^2/g$). The synthesis was performed in nitrogen environment and nonaqueous solvents due to the moisture- and air-sensitive nature of the vanadium precursor. The amount of the precursor, corresponding to the desired amount of vanadium oxide loading, and the solvent (Fisher ACS, 99.9% pure), corresponding to incipient wetness impregnation volume, were mixed thoroughly with the oxide support in a glovebox filled with nitrogen. The mixture was left standing for 16 h. The samples were then dried in flowing nitrogen at 393 K for 1 h and calcined in flowing air at 573 K for 1 h and at 773 K for 8 h.

The BET surface area data collected in Table 1 show that this calcination led to a significant loss of surface area with the CeO_2-supported samples while the other supports were more stable. The samples will be labeled *xy*-V-Z, with the approximate wt % V_2O_5 designated by *xy* and the support indicated by Z, e.g. 24-V-Al for 23.7 wt % V_2O_5/Al_2O_3. Samples with analogous composition may be further differentiated by indices a and b. The sample codes, actual vanadium contents, and surface densities of V atoms are summarized in Table 1. The monolayer coverage corresponds to ca. 8 V atoms/nm^2.

Methods. X-ray photoelectron and ion scattering spectra were measured with a Leybold surface analysis system equipped with X-ray and ion sources and an EA 10/100 electron (ion) analyzer

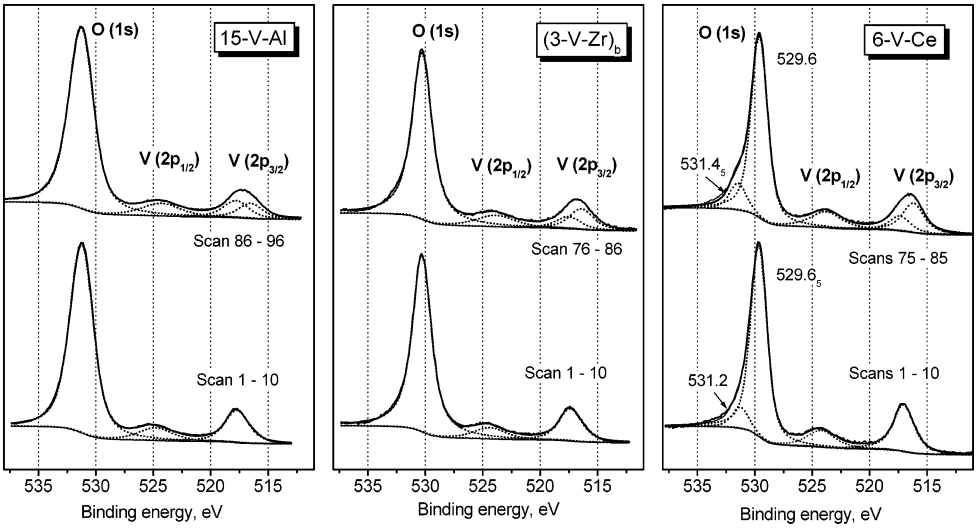

Figure 1. Evolution of XP spectra of supported V with extension of the data acquisition time. In the analysis of the final spectra, the V $(2p)_{1/2}$ signal was represented by only one line for the sake of simplicity.

with multichannel detection (Specs). The samples were recalcined in flowing synthetic air (20% O_2/N_2) at 730 K for 1 h before they were introduced into the spectrometer vacuum without further contact with the ambient humid atmosphere (in situ calcination). As-received samples were studied for comparison as well, but it should be noted that these samples had been calcined earlier as mentioned above and exposed to humidity-containing ambient atmosphere for an extended period of time. They will therefore be referred to as "stored in air".

XP spectra were recorded using Al Kα excitation (1486.6 eV, 12 kV × 20 mA), with the analyzer in pass-energy mode (pass energy = 35.5 eV). Data acquisition was performed in a sequential scheme, in which a sweep schedule covering the selected regions (O (1s) and V (2p), the major support line, C (1s)) was repeated many times, with all intermediate results being saved. This strategy allows for the inspection of the sample state at any time and for the proper selection of the data that are to be summed up for improvement of measurement statistics. Binding energies (BE) were primarily referenced to C (1s) = 284.5 eV, but in the tables typical BE values of the support cations obtained with the C (1s) calibration have been employed as secondary standards (Al (2p) = 74.0 eV, Zr ($3d_{5/2}$) = 182.2 eV, Ce ($3d_{5/2}$) = 882.6 eV, Nb ($3d_{5/2}$) = 207.1 eV). Further data reduction, which was performed with the software package MacFit,[18] included satellite deconvolution with user-specified satellite intensity parameters[19] and intensity evaluation. For this purpose, the V(2p), O(1s), and support cation lines (except Ce 3d) were fitted using Voigt-type line shapes in a routine that included the Shirley-type background[20] into the fitting, and the intensities were evaluated from the signal areas obtained. The Ce (3d) intensity was estimated by mere integration of the signal over a Shirley-type background. Due to the considerable width of this signal, the course of the background is difficult to establish, hence, the Ce (3d) intensities are of lower accuracy. Atomic ratios were calculated from intensity ratios by using Scofield interaction cross sections[21] together with an empirical response function of the spectrometer sensitivity to the photoelectron kinetic energy.

IS spectra were measured with 2000 eV He^+ ions (with the exception of a later analysis of 24-V-Al, performed with 1000 eV He ions, see Figure 7), and recorded with the analyzer in pass-energy mode (pass energy = 195 eV). ISS sputter series were performed by defining narrow scans over the lines of interest (V, support) and selecting an excitation current low enough to still produce spectra with tolerable noise level. The surface charge was removed with a flood gun. The source and the flood gun were allowed to stabilize with the sample withdrawn from the measurement position. After moving the sample under the He ion beam, the first scan was started within 5 s, with the V signal appearing after 30−50 s (depending on the atomic weight of the support cation) and the total length of a scan of typically 60−70 s. From estimates of the sample current produced by the source employed we believe that the short scans remove 0.05−0.1 of a monolayer per scan. Longer scans including the O signal were performed at the end of the sputter series where, however, the surface was already quite far from the original state. Signal intensities were estimated assuming the background to be linear.

Results

Typical XPS V (2p) spectra together with the nearby O (1s) lines are shown in Figure 1. The signal shapes at the start and the end of overnight data acquisition periods that had been initially scheduled to obtain high-quality spectra are compared. It is quite apparent that the V (2p) signal shape changes significantly, which indicates a reduction of surface V(V) species during the XPS measurement. By fitting the V ($2p_{3/2}$) XPS signals of the reduced samples with two lines of equal shape, the second state was found at a BE lower by 1.1−1.3 eV than the initial V(V) signal on the corresponding oxide support (typical V(V) binding energy data are given in Table 2). By reference to the literature, this can be used to identify the reduced state as V(IV) surface oxide species.[22−25]

XPS results showing the influence of the in situ calcination step on the spectra of the initially hydrated supported vanadium oxide species are presented in Table 2. In all cases the atomic ratio between V and the oxide support cation increases upon in situ calcination (dehydration). At the same time, a slight decrease of the Zr/O ratios takes place while the Al/O ratios remain constant. These trends, which indicate a redispersion of vanadia upon in situ calcination, are most pronounced with the ceria-supported samples, but they are here probably somewhat exaggerated because of the inaccurate integration of the Ce (3d) line (see prior discussion in the Experimental Section).

The binding energies of vanadium species on different supports are also compared in Table 2. No significant influence of the specific oxide support on the V (2p) binding energy can

TABLE 2: The Effect of Calcination of the XP Spectra of Supported V Catalysts

sample		binding energy, eV		atomic ratio	
code	treatment	V $2p_{3/2}$	O 1s	V/support[a]	support[a]/O
8-V-Al	stored in air	517.2	530.9	0.064	0.56
	calcined[b]	517.4	530.9_5	0.08_5	0.57
15-V-Al	stored in air	517.3	530.7_5	0.13	0.52
	calcined[b]	517.0	530.7_5	0.17	0.51
2-V-Zr	stored in air	517.2	530.2	0.11	0.43
	calcined[b]	517.4	530.2	0.13_5	0.38
$(3\text{-V-Zr})_b$	stored in air	517.1	530.1	0.20	0.37
	calcined[b]	517.3_5	530.3	0.28	0.34
2-V-Ce	stored in air	516.7	529.4 (532.0)	0.08_5	0.57
	calcined[b]	516.9	529.5 (531.7)	0.12	0.38
6-V-Ce	stored in air	516.8	529.6 (531.5)	0.22	0.46
	calcined[b]	517.2	529.6_5 (531.2)	0.52	0.30

[a] Al, Zr, or Ce. [b] 1 h, 730 K, synthetic air.

be noted: including the remaining samples, the values are found between 517.0 and 517.4 eV on alumina (additional sample: 24-V-Al), between 516.8 and 517.4 eV on ZrO_2 (additional samples: 1-V-Zr, $(3\text{-V-Zr})_a$, and 4-V-Zr), between 516.7 and 517.2. eV on CeO_2 (additional samples: 1-V-Ce, 3-V-Ce, and 5-V-Ce), and 517.3 eV on Nb_2O_5. It should be noted, however, that such a comparison is always influenced by the choice of the secondary BE standard, the support cation binding energy. Thus, for some of the oxide supports, the current reference BE data deviate significantly from those given in ref 26 (after recalibration to C (1s) = 284.5 eV − Al (2p) in γ-Al_2O_3 = 73.4 eV (vs 74.0 eV), Ce ($3d_{5/2}$) in CeO_2 = 881.6 eV (vs 882.6 eV); Zr ($3d_{5/2}$) in ZrO_2 = 181.9 eV (vs 182.2 eV); Nb ($3d_{5/2}$) in Nb_2O_5 = 207.3 eV (vs 207.1 eV)). The BE data used in this study are, however, well substantiated. Thus, the value taken for Al_2O_3 (74.0 eV) is between the average of 10 measurements with alumina-supported V and Mo surface oxide species (74.1 eV) and a measurement with the bare oxide support (73.8_5 eV), all referenced to C (1s) at 284.5 eV. The Ce ($3d_{5/2}$) BE of 882.6 eV for CeO_2 arises from an extended study with Ce-containing mixed oxides where binding energies were measured under reduced surface charge by heating the oxides during data acquisition.[27,28]

Additional minor O (1s) signals were observed with most V_2O_5/CeO_2 samples (see examples in Figure 1). They are possibly present in all spectra of ceria-supported vanadia, but their discrimination may have been prevented by considerable line broadening due to strong surface charging that sometimes occurred with freshly calcined catalysts. The BE of the minor O (1s) signal was between 531.2 and 532.0 eV, which is typical of OH groups. In the example shown in Figure 1, the O (1s) signal shape changes significantly during acquisition of the data, obviously in the course of the surface vanadium reduction. In the fit of the O (1s) signal shape, this is reflected by an upward BE shift of 0.3 eV of the minor peak relative to the major line. This is not a behavior that would be expected for a free OH group of the support. Moreover, the amount of free support OH groups should be very small and hardly detectable by XPS on the background of the lattice oxygen signal on a catalyst of surface vanadium oxide coverage above the monolayer capacity even if a small part of the support might have remained uncovered (see, however, below).

Figure 2 reports the dependence of the atomic ratio between vanadium and the support cation (determined by XPS) on the vanadium surface atom density for the V_2O_5/ZrO_2 and V_2O_5/CeO_2 series. As expected, there is a proportionality between these quantities up to the monolayer surface atom density, above which the slope of the curve changes significantly. From the intersections of the interpolated curves for submonolayer and for higher vanadium oxide contents, the monolayer capacity of Al_2O_3 can be determined to be 8.5 V atoms/nm^2, which is not far from the value of ca. 8 V atoms/nm^2 obtained from vibrational spectroscopy.

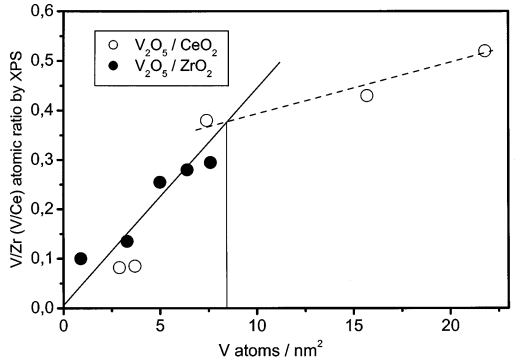

Figure 2. Relation between V/support ion atomic ratio and vanadium surface densities in the XP spectra of supported V_2O_5/ZrO_2 and V_2O_5/CeO_2 catalysts.

In Figure 3 examples of the ISS sputter series (6-V-Nb and 6-V-Ce) are presented. It can be seen that the support ion signals (Nb, Ce) are visible from the very first scan although their intensities are low. With sputtering time the support-ion signals grow dramatically as expected. With 6-V-Nb, the V peak intensity begins to decrease after an initial slight increase in the first two scans, but since the Nb peak intensity grows more rapidly the V/Nb ratio decays monotonically over the whole series (cf. also Figure 6). It was often observed that both signals had a lower intensity in the first one or two scans than the following ones. Therefore, conclusions were drawn mostly on the basis of intensity ratios.

In Figure 4, comparisons are made between the first ISS scans in the initial hydrated state and after dehydration by in situ calcination for several supported vanadium oxide catalysts. The differences noted already by XPS are even more pronounced in the IS spectra, which are more surface sensitive. The support peak is always visible in the first scan for the monolayer-supported vanadium oxide catalysts and the intensity ratio between the vanadium and the support signals increases with in situ calcination in all cases. The increase of the V/support ion ratio upon in situ calcination (dehydration) is very drastic in some cases, in other cases moderate. This certainly reflects that the initial state of the samples (precalcined, but stored in the ambient atmosphere) is not well defined because the rehydration was not performed under a controlled regime.

Analogously, it is possible that the photoreduction during XPS measurement may also affect the structure of the surface vanadate species: It has been reported in the earlier literature that supported Mo and V species aggregate upon reduction in hydrogen.[14,16,29,30] Therefore, IS spectra were taken also from samples that had not been exposed to X-rays before. During the extended XPS measurements documented in Figure 1, no significant changes were noted in the V-support ion atomic ratios. In Figure 5, the ISS intensity ratios between vanadium and the support ion signal (first scan) are plotted versus the surface vanadium density for the V_2O_5/ZrO_2 and V_2O_5/CeO_2 series. ISS data taken after extended XPS measurement are denoted by open symbols, ISS results measured without previous

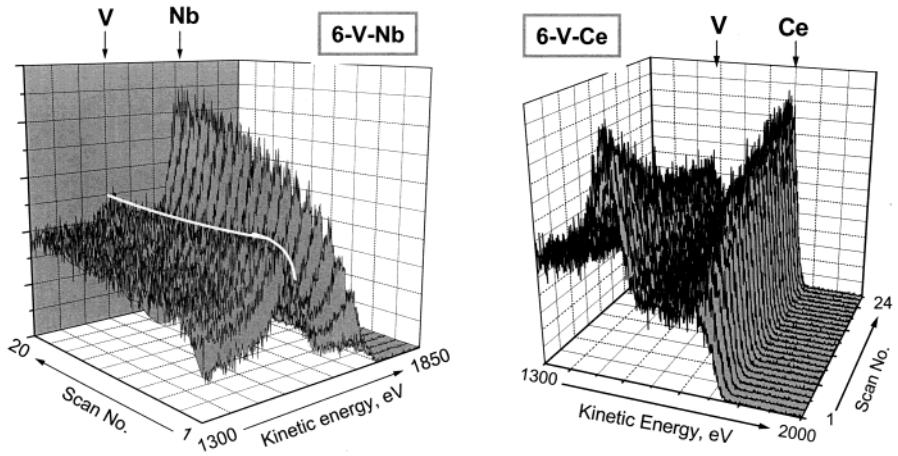

Figure 3. Examples for ISS sputter series: 6.1% V_2O_5/Nb_2O_5, 5.8% V_2O_5/CeO_2, both samples calcined, IS spectra recorded after previous XPS measurement.

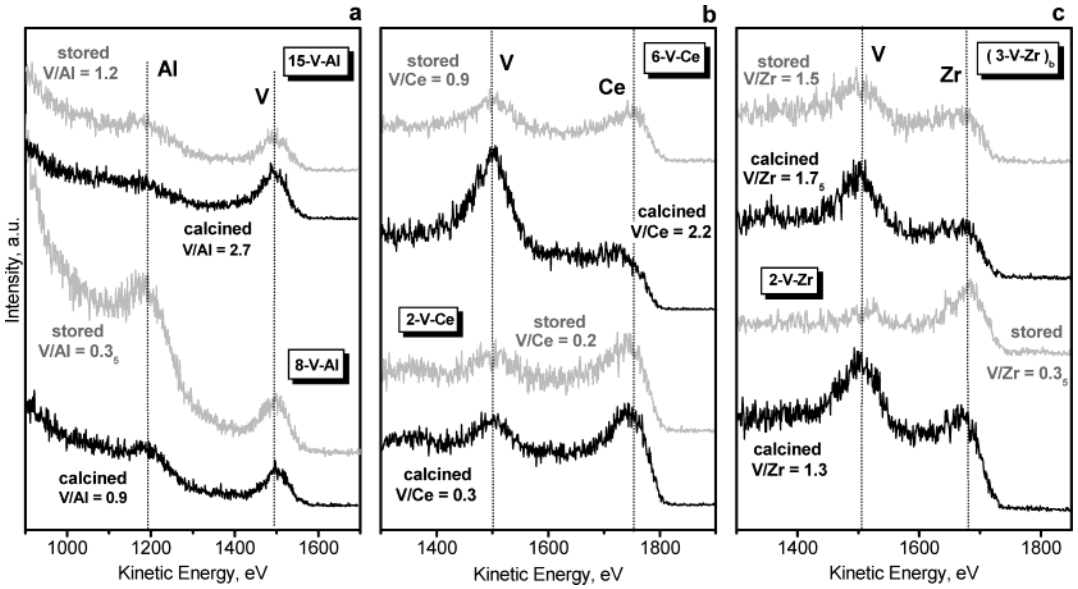

Figure 4. Influence of calcination on the IS spectra of supported V catalysts. Comparison of stored samples (i.e., calcined at 773 K, but stored in air) with samples immediately after calcination. All spectra recorded after previous XPS measurement: (a) V_2O_5/Al_2O_3 catalysts, (b) V_2O_5/CeO_2 catalysts, and (c) V_2O_5/ZrO_2 catalysts.

exposure of the samples to X-rays (and stray electrons) are given as solid symbols. Unlike the XPS intensities (Figure 2), the ISS intensity ratios are not proportional to the surface V density because at high coverage the support becomes more and more invisible to the scattered He ions. There is a significant increase of the initial V/Ce (or V/Zr) ratio when ISS is measured without previous XPS analysis, but there was never a case where the support ion signal was completely missing in the first scan. This observation does not necessarily indicate an incomplete shielding of the support at the theoretical monolayer coverage due to the formation of three-dimensional aggregates because it may have resulted from the erosion of some vanadium in the first seconds of the experiment before the kinetic energy sweep reaches the location of the support ion signal.

This question can be decided when the trend of the area ratio between support ion and vanadium with increasing scan number is extrapolated to the start of the experiment. When the support is completely covered by the supported vanadia species this extrapolation has to go through the origin of the coordinate system. Figure 6 shows the extrapolation for supported V_2O_5/ZrO_2, V_2O_5/CeO_2, and V_2O_5/Nb_2O_5 catalysts with loadings near or at the theoretical monolayer surface coverage (3-V-Ce, (3-V-Zr)$_b$, 4-V-Zr, 6-V-Nb) or above (5-V-Ce, 6-V-Ce). Figure 7 gives analogous data for the V_2O_5/Al_2O_3 system (15-V-Al and 24-V-Al). In the diagrams, sputter series taken after XPS measurements (open symbols) are again compared with runs on samples that had not been exposed to X-rays before (solid symbols). It becomes obvious from these figures that in most supported vanadia catalyst systems, the surface vanadium oxide layer is dense at the beginning of the run: the extrapolation of the support ion/V area ratio goes through the origin in all cases except 3-V-Ce and the V_2O_5/Al_2O_3 catalysts where very small intercepts were found. In the first case, it should be noted that the ceria support is more reactive than the remaining ones, tending to the formation of bulk $CeVO_4$, which would decrease the amount of vanadium species in the outermost surface layer. The significant loss in BET surface area with the calcined V_2O_5/CeO_2 catalysts (Table 1) may suggest that this has occurred to some extent. Indeed, at higher vanadia content, the surface was found to be completely covered by surface vanadium oxide species (see samples 5-V-Ce and 6-V-Ce, Figure 6).

The V_2O_5/Al_2O_3 system, however, appears to differ from the remaining ones: even for 24-V-Al (almost 10 V atoms/nm^2), the sputter series cannot be extrapolated to V/Al = 0 at zero sputtering time (Figure 7a). This is true despite some anomalies in the sputter series recorded with this catalysts, which nicely

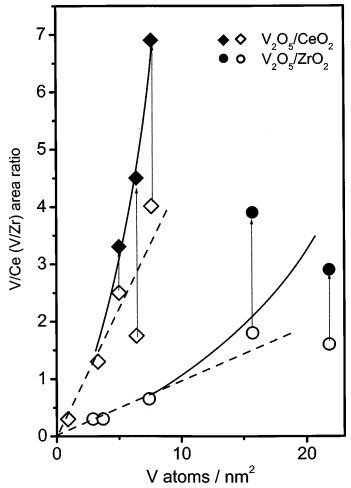

Figure 5. Relation between V/support ion intensity ratio and vanadium surface densities in the IS spectra (first scan) of supported V_2O_5/ZrO_2 and V_2O_5/CeO_2 catalysts. All samples calcined prior to measurement. Open symbols, IS spectra taken after XPS measurements; solid symbols, IS spectra taken with fresh samples.

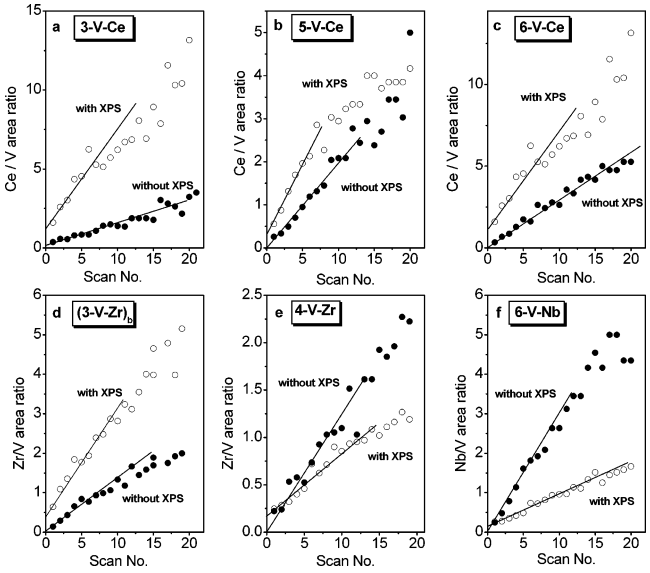

Figure 6. Development of support ion/V intensity ratio in the ISS sputter series with supported vanadia catalysts. Comparison of measurements after previous XPS analysis (open symbols) and measurements with fresh sample (solid symbols): (a) 2.6% V_2O_5/CeO_2, (b) 4.7% V_2O_5/CeO_2, (c) 5.8% V_2O_5/CeO_2, (d) 3.3% V_2O_5/ZrO_2, (e) 4.0% V_2O_5/ZrO_2, and (f) 6.1% V_2O_5/Nb_2O_5.

illustrate the experimental problems with the V−Al system: The Al signal appears on the slope of the intense O signal. Therefore, it is very difficult to determine a realistic background for the Al signal, and the values determined by assuming a linear background underestimate rather than overestimate the Al intensity. Any deterioration of the resolution as occurred in the experimental series between scans 5 and 10 (Figure 7b) strongly affects the areas determined (Figure 7a). It can be assumed, however, that the tendency of growing Al/V ratio observed with ongoing sputtering reflects the uncovering of the Al_2O_3 surface correctly. Even if this trend is aligned to the first data point, it does not extrapolate the series to the origin (Figure 7a). Notably, in an earlier study with supported Mo catalysts a nonzero Al/Mo ratio was obtained in the extrapolation of the Al/Mo area ratios for a supported MoO_3/Al_2O_3 catalyst with Mo surface atom density at monolayer limit while the support turned out to be completely covered in an analogous MoO_3/TiO_2 catalyst.[31]

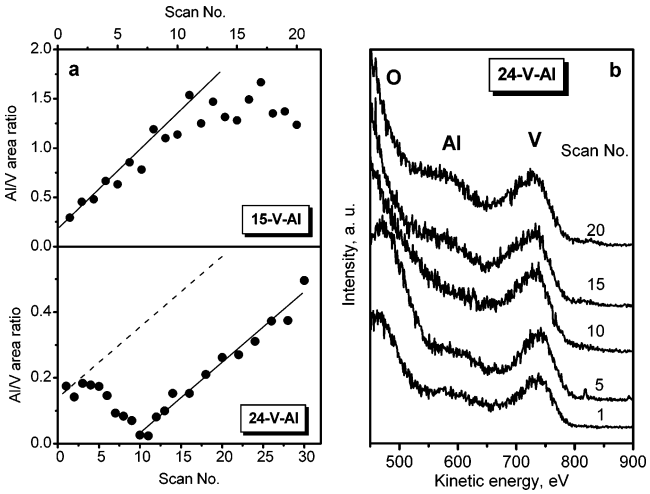

Figure 7. ISS sputter series with supported V_2O_5/A_2O_3 catalysts. (a) Development of support ion/V intensity ratio in samples with surface V density near and above theoretical monolayer capacity (spectra recorded without previous XPS analysis) and (b) demonstration of spectral effects leading to anomaly in the sputter series; spectra recorded with 1000 eV He ions.

Discussion

In the present study, it has been found by XPS as well as by ISS that the intensity ratios between the V signal and that of the support increase significantly after dehydration by in situ calcination in air at 730 K. This can be considered as supporting the view that the vanadia was detached from the oxide support surface and clustered in the hydrated samples ($V_{10}O_{25}\cdot nH_2O$), forming surface vanadia species only upon dehydration. However, alternative explanations have to be considered as well, e.g. different influences of possible overlayers in the hydrated and the calcined states. Indeed, residual water and adventitious carbon should be present in larger amounts on the hydrated than on the freshly calcined samples. For carbon, this is confirmed by the trends of the C (1s) line intensity, which is always lower after calcination. The frequently observed increase of the overall intensity of the IS spectra during the first scans might also be attributed to the removal of adsorbed molecules.

On the other hand, the overlayer hypothesis can provide measurable effects in the V/support ion ratios measured by the less surface sensitive XPS only if these layers are thick or predominantly located on the vanadium species. The presence of multilayers of adsorbed water is highly unlikely in UHV, and disproved by the absence of O (1s) signals at >532 eV, where molecularly adsorbed water is usually found.[26] Multilayer adsorbates should also prevent the detection of ISS signals of vanadium and the support lines from the very first scan. The presence of an adsorbate monolayer exclusively or preferentially on vanadium should give rise to intermediate *in*creases of the V/support ion ISS intensity ratio. With the exception of the anomalous case of 24-V-Al (vide supra, Figure 7), this has never been observed with any sample, and the V/support ion ratios had a monotonically decreasing trend in all cases. Hence, the formation of the surface vanadia species upon in situ calcination, which includes spreading of the aggregated vanadia phase, is the best explanation of the XPS and ISS intensity trends observed. A similar phenomenon is known from the earlier literature for supported MoO_3/Al_2O_3 catalysts.[14,32] We have, however, performed our study with "initial" samples that had already undergone a calcination at a higher temperature than applied prior to surface analysis. Therefore, our results support the view that the surface metal oxide species are not stable

toward moisture in the ambient atmosphere, which leads to the re-formation of an aggregated hydrated surface vanadium oxide phase.

Our study has confirmed earlier reports about the reduction of supported V^{5+} species under X-ray irradiation.[16,17] The reduction product is V^{4+}. The clustering of the V phase during photoreduction has been detected by ISS (Figure 6) but not by XPS. In fact, the detection of significant changes in the IS spectra was a surprise because of the very mild reduction conditions that should not favor the mobility of the surface vanadia species on the support. Indeed, the clustering tendency is weak since it does not lead to significant changes in XPS. On the other hand, it is existent and clearly identified by ISS.

The extrapolation of the support ion/vanadium intensity ratio to the beginning of the experiment proved that the support ions are not exposed to vacuum or gas phase when vanadium is supported in theoretical monolayer coverage or above on CeO_2, ZrO_2, and Nb_2O_5 supports (see Figure 6). A slight initial Ce intensity in $(3\text{-V-Ce})_b$ may be due to the lower vanadia loading of this surface (vide supra, possible bulk incorporation of V species during calcination). The results confirm the view that the surface vanadia species form a complete monolayer on the oxide support before growing into the third dimension.[1] It is, however, at variance with several other reports in the literature (vide supra). The structural effects of in situ calcination (dehydration) and photoreduction demonstrated in this paper give indications for possible reasons of this apparent difference: the correct result can only be obtained with in situ calcined and dehydrated samples that have not been used for prior XPS measurements. Furthermore, it was necessary to also record the sputtering series under conditions with as low as possible erosion per scan, and only the extrapolation of this series to zero sputtering time resulted in the conclusion that the support cations are indeed completely covered by the surface vanadia monolayer. Another possible reason for the disagreement of results may be the use of improper precursors or routes for catalyst preparation.

The above conclusion, however, does not hold for alumina as shown in Figure 7. The results with this support differ from the previous cases also in the observation that the vanadium signal remains visible even after extended sputtering while it can be almost completely removed in the other oxide supports (compare support ion/V intensity ratios achieved in the sputter series documented in Figures 6 and 7). These differences may be a consequence of the largely different BET surface areas of the supports involved (see Table 1). Complete removal of the surface vanadia by prolonged sputtering can only be expected for flat surfaces, with the surface normal pointing into the analyzer direction. High surface-area supports possess strongly curved surfaces, most of which have other orientations to the analyzer. As a consequence, the changes in the V and Al signals are very gradual, and a considerable V intensity arising from surfaces at various angles from that normal to the analyzer direction remains. Therefore, it is clear that the initial Al/V intensity ratio of ca. 0.2 (Figure 7) corresponds to a low Al exposure although a quantitative value for the vanadia coverage cannot be derived. Figure 6 shows that vanadium oxide monolayers are dense on surfaces of lower curvature (primary particle diameters of $d_p = 23-30$ nm may be estimated from the BET surface areas of the bare supports (cf. the Experimental Section) with the equation $d_p = 6/(\rho A_{BET})$ assuming spherical particles and densities ρ of 6, 7.3, and 4.5 g cm^{-3} for ZrO_2, CeO_2, and Nb_2O_5, respectively). However, support ions may be exposed to the gas phase at strong curvature, edges, or kinks because a dense cover on the convex side of a curved surface has to be slightly larger than the surface itself where the density of sites capable of anchoring surface vanadate species does not increase. This would imply that the monolayer is completely built up but not completely dense because of the surface curvature (Al_2O_3 primary particle diameter estimated: 8 nm (ρ-(γ-Al_2O_3) = 3.4 g cm^{-3})). It should be noted, however, that the Al cations detected by the small He probe in ISS cannot be identified in experiments with chemical probes (methanol chemisorption).[33]

A final remark refers to the BE shift of the minor O (1s) signal during photoreduction of the monolayer sample 6-V-Ce (cf. Figure 1). The binding energy of this minor contribution is in a region where support OH group signals are expected, but the BE shift suggests that the oxygen is associated with vanadium. Indeed, given the dense vanadate coverage detected on this sample by ISS (Figure 6), Ce-OH groups can be safely rejected. Alternatively, the signals could arise from oxygen in groups on the vanadia multilayer in this sample (V−OH groups or lattice oxygen), but the latter is unlikely because in V_2O_5, the O (1s) signal appears at ca. 530 eV. Finally, the signal could be assigned to oxygen bridges between vanadium and the support, which originate from the OH groups previously present on the surface. At present, it is difficult to discriminate between the remaining choices (V−OH or V−O−Ce bridges), hence, more effort will be required to establish if we have a chance here to detect oxygen bridging between the support and the supported layer in the V/Ce/O system. Unfortunately, the O (1s) BE of bulk oxygen in the remaining supports is higher so that there is hardly any chance to find out if a similar state is superimposed.

Conclusions

In situ calcination and dehydration of supported vanadia catalysts leads to significant intensity increases of the V signals relative to the cation signals of the oxide support in surface analytical studies by XPS and ISS. These intensity increases, which were obtained upon recalcination of calcined samples that had been stored in contact with the ambient and humid atmosphere for prolonged periods, indicate the formation of a dehydrated surface vanadia monolayer on the oxide supports from hydrated aggregates upon in situ calcination. The vanadia clusters reform during interaction with moisture. Surface vanadium oxide species are reduced during prolonged exposure to the X-rays of a (nonmonochromatized) X-ray source. Despite the mild reduction conditions, this reduction leads to clustering of the vanadate, which is detectable by ISS but not by XPS. It was found that meaningful conclusions from ISS measurements require the performance of sputter series and their extrapolation to zero time. On this basis, it was demonstrated that supported V_2O_5/CeO_2, V_2O_5/ZrO_2, and V_2O_5/Nb_2O_5 catalysts with a surface vanadia loading corresponding to the monolayer coverage or above form a close-packed vanadia monolayer on the oxide support. However, a small number of Al ions are exposed on the V_2O_5/Al_2O_3 catalyst at theoretical monolayer coverage, which was attributed to the high specific surface area and the highly curved surface of the alumina support.

Acknowledgment. I.E.W. and L.E.B. gratefully acknowledge the United States Department of Energy, Basic Energy Sciences (Grant DEFG02-93ER14350), for financial assistance. I.E.W. dedicates this paper to the memory of Dr. Robert Beyerlein, who was formerly in charge of the catalysis programs at DOE.

References and Notes

(1) Deo, G.; Wachs, I. E.; Haber, J. *Crit. Rev. Surf. Chem.* **1994**, *4*, 141.
(2) Banares, M. A.; Wachs, I. E. *J. Raman Spectrosc.* **2002**, *33*, 359.
(3) Wachs, I. E. *Catal. Today* **1996**, *27*, 437.
(4) Knözinger, H. In *Proceedings of the 9th International Congress on Catalysis, Calgary 1988*; Phillips, M. J., Ternan, M., Eds.; The Chemical Institute of Canada: Ottawa, Canada, 1988; Vol. 1, p 20.
(5) Centi, G. *Appl. Catal. A* **1996**, *147*, 267.
(6) Eberhardt, M. A.; Houalla, M.; Hercules, D. M. *Surf. Interface Anal.* **1993**, *20*, 766.
(7) Fiedor, J. N.; Houalla, M.; Proctor, A.; Hercules, D. M. *Surf. Interface Anal.* **1995**, *23*, 234.
(8) Vaidyanathan, N.; Houalla, M.; Hercules, D. M. *Catal. Lett.* **1997**, *43*, 209.
(9) Vaidyanathan, N.; Houalla, M.; Hercules, D. M. *Surf. Interface Anal.* **1998**, *26*, 415.
(10) Zingg, D. S.; Makovsky, L. E.; Tischer, R. E.; Brown, F. R.; Hercules, D. M. *J. Phys. Chem.* **1980**, *84*, 2398.
(11) Gunter, P. L. J.; Niemantsverdriet, J. W.; Ribeiro, F. H.; Somorjai, G. A. *Catal. Rev.-Sci. Eng.* **1997**, *39*, 77.
(12) Taglauer, E.; Knözinger, H. *Phys. Status Solidi B* **1995**, *192*, 465.
(13) Salvati, L., Jr.; Makovsky, L. E.; Stencel, J. M.; Brown, F. R.; Hercules, D. M. *J. Phys. Chem.* **1981**, *85*, 3700.
(14) Houalla, M.; Kibby, C. L.; Eddy, E. L.; Petrakis, L.; Hercules, D. M. *Proceedings, 8th International Congress on Catalysis, Berlin 1984*; VCH Weinheim: Weinheim, Germany, 1984; Vol. V, p 147.
(15) Sazo, V.; Gonzalez, L.; Goldwasser, J.; Houalla, M.; Hercules, D. M. *Surf. Interface Anal.* **1995**, *23*, 367.
(16) Eberhardt, M. A.; Proctor, A.; Houalla, M.; Hercules, D. M. *J. Catal.* **1996**, *160*, 27.
(17) Meunier, G.; Mocaer, B.; Kasztelan, S.; LeCoustumer, L. R.; Grimblot, J.; Bonelle, J. P. *Appl. Catal.* **1986**, *21*, 329.
(18) Boyen, H.-G. *MacFit*, Surface Analysis Software Package; University of Basle: Basle, Switzerland.
(19) Wark, M.; Koch, M.; Brückner, A.; Grünert, W. *J. Chem. Soc., Faraday Trans.* **1998**, *94*, 2033.
(20) Shirley, D. A. *Phys. Rev. B* **1972**, *5*, 4709.
(21) Scofield, J. H. *J. Electron Spectrosc. Relat. Phenom.* **1976**, *8*, 129.
(22) Heber, M.; Grünert, W. *J. Phys. Chem. B* **2000**, *104*, 5288.
(23) Poelman, H.; Fiemans, L. *Solid State Commun.* **1994**, *92*, 669.
(24) Chiarello, G.; Robba, D.; De Michele, G.; Parmigiani, F. *Appl. Surf. Sci.* **1993**, *64*, 91.
(25) Christmann, T.; Felde, B.; Niessner, W.; Schalch, D.; Scharmann, A. *Thin Solid Films* **1996**, *287*, 134.
(26) Wagner, C. D. In *Practical Surface Analysis*, 2nd ed.; Briggs, D., Seah, M. P., Eds.; Wiley: Chichester, UK, 1990; Vol. 1, Appendix 5.
(27) Heber, M. Ph.D. Thesis, Ruhr-Universität Bochum, Bochum, Germany, 1999.
(28) Wolf, D.; Heber, M.; Grünert, W.; Muhler, M. *J. Catal.* **2001**, *199*, 92.
(29) Grünert, W.; Stakheev, A. Y.; Mörke, W.; Feldhaus, R.; Anders, K.; Shpiro, E. S.; Minachov, K. M. *J. Catal.* **1992**, *135*, 269.
(30) Liu, H. C.; Weller, S. W. *J. Catal.* **1980**, *66*, 65.
(31) Briand, L. E.; Tkachenko, O. P.; Guraya, M.; Wachs, I. E.; Hu, H.; Grünert, W. *Surf. Interface Anal.* **2004**, *36*, 238.
(32) Margraf, R.; Leyrer, J.; Knözinger, H.; Taglauer, E. *Surf. Sci.* **1988**, *201*, 603.
(33) Burcham, L. J.; Briand, L. E.; Wachs, I. E. *Langmuir* **2001**, *17*, 6164.